Towards Determining Wind Disturbance Levels for an Urban Air Mobility Aircraft Through Simulation-Based Flight Testing

Nithya D S
PhD student
Politecnico di Milano
RMIT University
Milan, Italy

Agata Rylko
PhD student
Politecnico di Milano
Milan, Italy

Vincenzo Muscarello
Senior Lecturer
RMIT University
Melbourne, VIC, Australia

Man Liang
Senior Lecturer
RMIT University
Melbourne, VIC, Australia

Giuseppe Quaranta
Professor
Politecnico di Milano
Milan, Italy

ABSTRACT

Urban Air Mobility (UAM) aircraft performance will be affected by the prevalent microscale wind disturbances within cities. These localized wind effects amplify operational risks and pose a challenge for the flight testing of UAM aircraft. One way to overcome these hindrances related to microscale wind conditions is through simulation-based flight tests. Thus, this paper proposes a simulation-based methodology to determine the level of wind disturbance for UAM aircraft by assessing the risks of trajectory deviation or the risk of degradation of Handling Quality ratings. In addition, a case study will be presented using the proposed methodology, where a lift+cruise drone, representing a UAM aircraft, performs vertical landing behind an isolated tall building. The study analyzes the deviations of the aircraft trajectory for different microscale wind conditions to provide information on the associated levels of wind disturbance.

INTRODUCTION

Buildings and other obstacles in urban environments disrupt the wind flow, creating different flow regions with increased turbulence. These effects are highly dynamic and localized, as wind characteristics vary depending on the urban landscape, time, and the conditions of the inflow wind. Such wind phenomena will impact Urban Air Mobility (UAM) aircraft performance, amplify operational safety risks (Ref. 1), and consequently affect the certification process of these aircraft as flight testing over cities is expensive, time-consuming, and fraught with risks that require comprehensive mitigation strategies (Ref. 2).

Many UAM aircraft manufacturers conduct flight tests in remote areas or open fields, where wind conditions differ significantly from those in urban environments. While such evaluations generate sufficient performance data to define the operational limits and obtain certification as per the existing compliance standards (Ref. 3), they fail to quantify the performance deviation risks associated with operating these aircraft in microscale wind conditions. Moreover, due to varying UAM aircraft configurations, operational environments (cities), and localized wind conditions, aircraft performance in one environment may not be the same as in another. This emphasizes the need for studying UAM aircraft performance deviations across different operational environments to determine wind disturbance levels. Addressing this challenge remains difficult due to the complexities involved in flight testing over densely populated cities. A viable approach to overcoming the aforementioned challenges related to flight testing, microscale wind conditions, and aircraft performance is to conduct simulation-based flight tests that incorporate realistic microscale wind data.

Unlike at high altitudes, observational wind data at low altitudes is scarce, as placing sensors is both logistically challenging and impractical due to the highly dynamic and turbulent nature of the wind. Thus, an alternative approach to obtaining realistic wind data for flight simulations is to model wind flow across urban landscapes numerically. Various methods exist to model microscale wind flows, but not all are suitable for every UAM application or study (Ref. 4). That is, CFD techniques like LES offer high accuracy and resolution but limit domain size and require extensive computation time. These factors make CFD impractical for quantifying wind-related UAM aircraft performance deviations through simulation-based flight tests. However, despite such limitations, most wind turbulence models used in the UAM community are CFD-based or spectral models like Von Kármán, which do not accurately represent low-altitude wind conditions. For instance, a group of researchers from NASA has studied the impact of varying wind speed and direction on the trajectory deviation of an Uncrewed Aerial Vehicle (UAV) (Ref. 5). Their study quantifies the probability of trajectory deviation for different wind speeds and directions by assuming that the turbulence follows the Von Kármán spectrum. Along the same lines, the authors in (Ref. 6) use the Markov Chain Monte Carlo method with an eVTOL flight dynamics model to estimate the probability of exceeding performance requirements outlined in EASA's Special Condition - Vertical Takeoff and Landing (SC-VTOL) standards during landing. They vary several parameters, including wind speed, direction, air temperature, pressure, and the Von Kármán turbulence length scale, to estimate results. However, it remains unclear whether the wind values used are representative of a realistic urban environment. On the contrary, the authors in (Ref. 7) investigate how a fixed-wing aircraft responds to microscale wind conditions behind a stadium during its transition from cruise to landing. While their study distinguishes the aircraft's response to microscale wind fields generated by LES and wind Reduced Order Models (ROMs), it does not examine how varying inflow wind conditions in the operational area affect the aircraft's dynamic response to define the wind disturbance levels. On the whole, it can be inferred that further research is needed to devise an efficient methodology for assessing wind disturbance levels that cause performance deviations in UAM aircraft.

In response to the existing challenges and gaps, this paper proposes an efficient methodology to determine the wind disturbance levels for a UAM aircraft through simulation-based flight tests. Additionally, a case study of a UAM aircraft landing vertically into a microscale wind field behind an isolated tall building is simulated using the proposed methodology. The data from the simulation is then assessed to determine the probability and severity of aircraft performance deviation during the vertical landing phase in the assumed scenario, to quantify the wind disturbance levels.

METHODOLOGY

The overall methodology involves the use of a Stochastic microscale Wind Model (SWM) and a MATLAB-Simulink-based flight simulator, embedded within a Monte-Carlo simulation framework. SWM is a custom microscale wind modeling approach that represents wind velocity fields using the Reynolds decomposition technique, where the total velocity is expressed as the sum of its mean component and turbulent fluctuations. Hence, it combines a highly-parameterized steady-state wind solver, QUIC-URB or QES-Winds (Refs. 8, 9), with a turbulence generator, TurbSim (Ref. 10). QUIC-URB (Quick Urban and Industrial Complex - URBan) and QES (Quick Environmental Simulation)-Winds are empirical, diagnostic, steady-state, mass-consistent wind solvers that are developed by researchers at Los Alamos National Laboratory and the University of Utah, respectively. Unlike traditional CFD methods, QUIC and QES parametrize the different flow regions around buildings using obstacle dimensions—length (L), width (W), height (H)—as well as shape, inlet wind direction, and speed to estimate wind velocity fields. These solvers generate 3D wind flow field data for high-resolution simulation domains within minutes to seconds on standard desktop or laptop computers. Meanwhile, TurbSim is a stochastic, full-field inflow turbulence generator developed by researchers at the National Renewable Energy Laboratory (NREL). It offers users the flexibility to choose turbulence spectral models and import user-defined wind profiles from steady-state solvers like QUIC or QES to simulate time-series turbulent fluctuations to produce microscale wind velocity data.

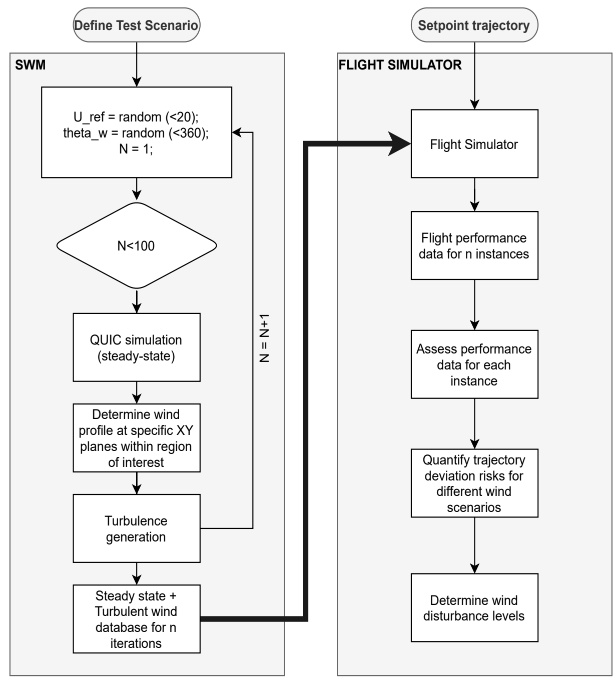

Figure 1. High-level workflow of the methodology to determine wind disturbance levels for a UAM aircraft through simulation-based flight testing.

As shown in Figure 1, firstly, a UAM aircraft operational scenario is defined. Subsequently, a Monte Carlo simulation is initiated by invoking the SWM to generate microscale wind data by varying the reference inlet wind speed (U_{ref_i}) and direction (θ_{w_i}). This process is repeated for n iterations, yielding a diverse database of urban microscale wind disturbances, each representing a unique inflow configuration within the chosen operational context. These wind disturbance samples are then integrated with the flight simulator to generate aircraft performance data corresponding to each of the n instances. The resultant flight performance database is analyzed to evaluate trajectory deviations and their probabilities under varying wind disturbances, while also identifying scenarios with a significant risk of Loss of Control (LOC). Finally, the insights gained from this analysis are leveraged to define the wind disturbance levels for the aircraft.

CASE STUDY: UAM AIRCRAFT VERTICAL LANDING IN URBAN WIND FIELD

To demonstrate the methodology outlined in the previous Section, the case study in this section is based on a simplified operational scenario similar to that in (Refs. 11, 12). An eVTOL performs a vertical landing from an altitude of 40 meters at a descent rate of 1 m/s behind an isolated building with dimensions $L = B$ and $H = 2L$.

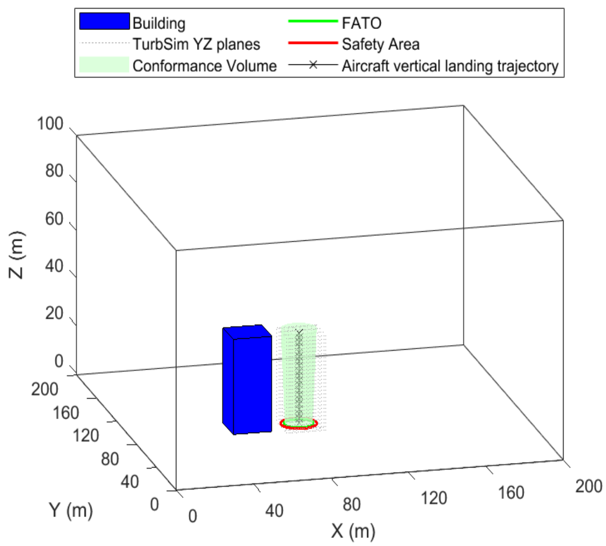

Figure 2. Pictorial representation of the operational scenario used for the case study.

Figure 2 shows the entire simulation domain employed within the Monte Carlo Simulation framework. The domain encompasses the isolated building, the microscale wind field simulation planes (or TurbSim YZ planes), and the vertical landing trajectory of the eVTOL aircraft, which is heading north with a yaw of 0 degrees at 40 m altitude. The landing point is situated 15 m downstream from the rear face of the building and is aligned with the center of the Touchdown and Lift-Off Area (TLOF). The Final Approach and Takeoff Area (FATO), also referred to as the 3D conformance volume, has a base radius of 7.5 m with a slope of 5% and is supplemented by a safety area (SA) with a radius of 9 m in accordance with the EASA vertiport design standards (Ref. 13).

The flight simulator used in this study models a lift+cruise eVTOL drone (see Figure 3 with a mass of 7.1kg, a wingspan of 3.12m, and 10 propellers (8 for vertical lift, 2 for forward flight), developed at the Aerospace Systems and Controls Laboratory (ASCL) of Politecnico di Milano, Italy. It simulates rigid-body dynamics using nonlinear equations of motion and a quasi-linear parameter-varying (qLPV) aerodynamic model. The simulator supports both multicopter and fixed-wing flight modes for transitions between vertical and forward flight. This study uses the multicopter mode, where aerodynamic forces on the wings are neglected during vertical descent, and total thrust and torque are computed from wind tunnel–derived propeller coefficients. A custom PX4-

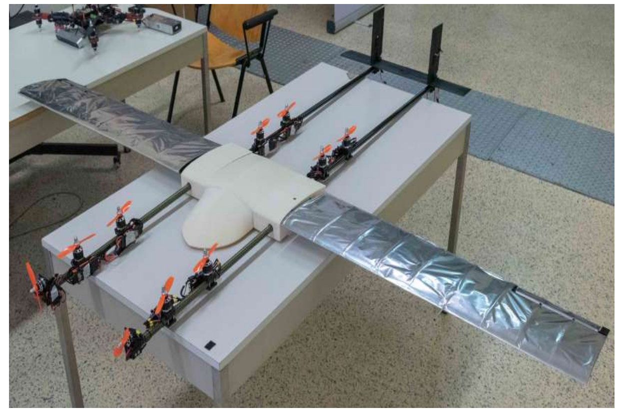

Figure 3. Lift+cruise eVTOL drone (Ref. 14).

based autopilot employing cascaded PID loops provides position, velocity, and attitude control. For further details on the simulator, see Refs. 14–20.

The Monte Carlo simulation consists of 100 iterations to capture a broad range of wind conditions affecting eVTOL operations. For each iteration, the inlet wind speed (below 20 m/s) and direction (0°–360°) are randomly varied to first generate steady-state wind flow fields using QUIC-URB. Then, the resultant steady-state wind data is post-processed to determine the wind flow profiles at the TurbSim YZ planes, covering the FATO behind the building. These profiles serve as the input to the TurbSim simulation, which produces the full-field microscale wind velocity data[1] for the flight simulations. Furthermore, the entire Monte Carlo simulation framework is automated using a combination of MATLAB and Python scripts, and executed on a standard laptop equipped with an 11th Gen Intel processor featuring 4 cores and a base speed of 2.80 GHz. The total time required to obtain flight performance data for all 100 iterations is approximately 30 hours, with around 27 hours dedicated to wind data generation and 3 hours to real-time flight simulations.

Trajectory deviation analysis

A comprehensive dataset totaling 40 GB was collected across 100 Monte Carlo simulation iterations, comprising 33 GB of high-resolution microscale wind disturbance data and 7 GB of flight performance data. To facilitate systematic analysis of trajectory deviation within this extensive dataset, the aircraft positional data from all iterations were aggregated and categorized into the following 4 distinct classes:

1. **Conforming Trajectories:** These are trajectories that remain entirely within the predefined conformance volume throughout the descent phase and successfully reach the designated landing point at the stipulated 40 s descent time. Thus such trajectories represent nominal behavior with negligible deviations.
2. **Temporally Non-Conforming Trajectories:** Trajectories falling within this category adhere to the spatial conformance constraints throughout the descent but fail to

[1] Detailed information on the wind simulation setup is provided in (Ref. 12).

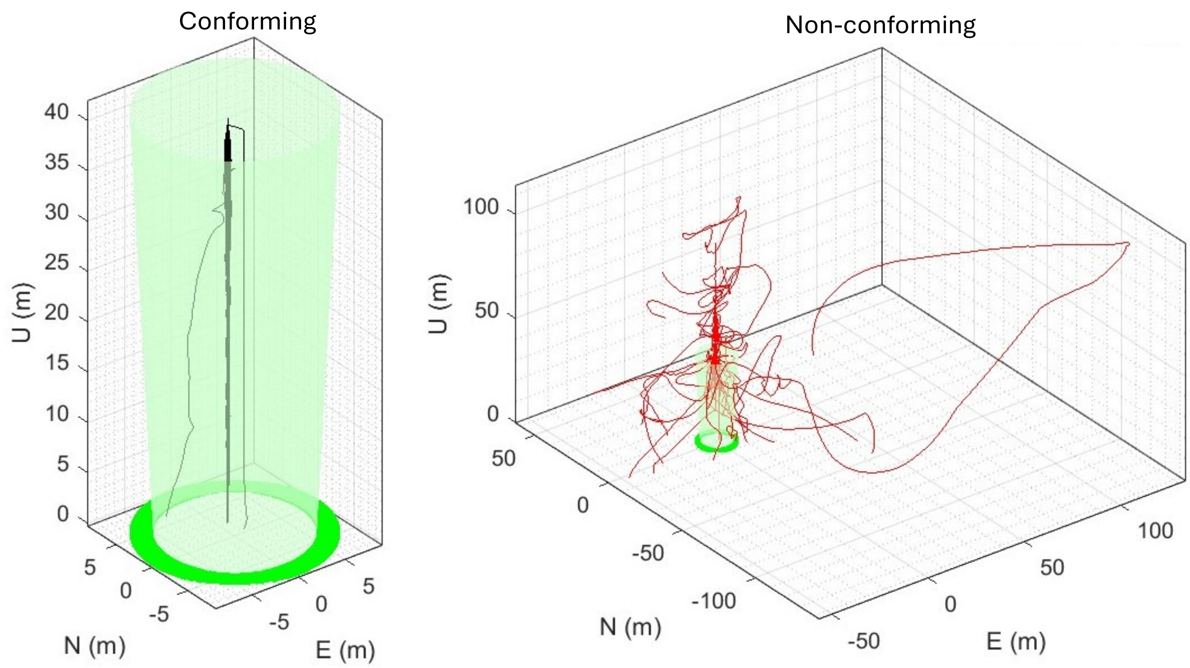

Figure 4. Conforming vs. non-conforming trajectories.

meet temporal conformance. That is, these trajectories are characterized by the aircraft maintaining an altitude greater than 1 m above the ground at the 40s timestamp, indicating a delay in descent due to wind disturbances.

3. **Non-Conforming Trajectories:** This class includes any trajectory that, at any point during the descent, diverges beyond the boundaries of the conformance volume. Such deviations may occur due to controller transient responses to wind disturbances, and they signify a failure to maintain the prescribed descent corridor.
4. **Loss of Control (LOC):** These cases represent the most severe deviations, wherein the flight controller fails to compensate for the perturbations induced by wind disturbances, resulting in a complete loss of control authority and rendering the trajectory irrecoverable within mission constraints.

Out of the 100 Monte Carlo iterations, a total of 11 trajectories were classified as conforming, while 12 were identified as temporally non-conforming. 36 trajectories exhibited spatial deviations and were categorized as non-conforming, and the remaining 41 iterations resulted in control loss. As depicted in Figure 4, several of the non-conforming cases demonstrate significant spatial deviations–some exceeding 50 m beyond the defined conformance volume. These deviations underscore potential operational safety concerns, such as collision risk, arising from the combined effects of microscale wind disturbances and the limited ability of the controller to compensate during the vertical descent phase in a building vicinity.

Figure 5 is a polar scatter plot showing the distribution of Monte Carlo inputs for the simulation domain–the incidence wind speed and direction–across 100 iterations, categorized

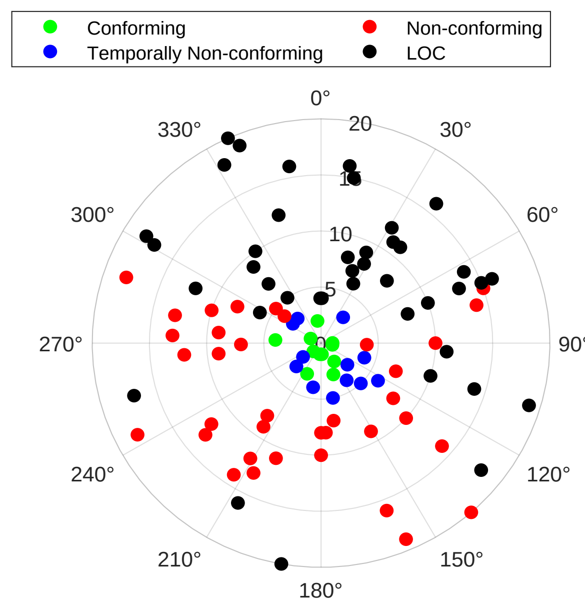

Figure 5. Monte Carlo simulation inputs grouped by trajectory compliance classification.

into the 4 distinct trajectory classes. It can be observed that the conforming trajectories consistently exhibit incidence wind speeds ranging from 0 to 5 m/s, with directions predominantly falling between 120 and 210 degrees, indicating a prevailing flow towards the positive Y-axis or the tail of the aircraft. The temporally non-conforming cases have a slightly elevated incidence wind speed when compared to the conforming cases. In contrast, non-conforming trajectories are characterized by significantly higher wind speeds, between 5 and 15 m/s, with a broad predominant wind direction spanning 90 to 270 de-

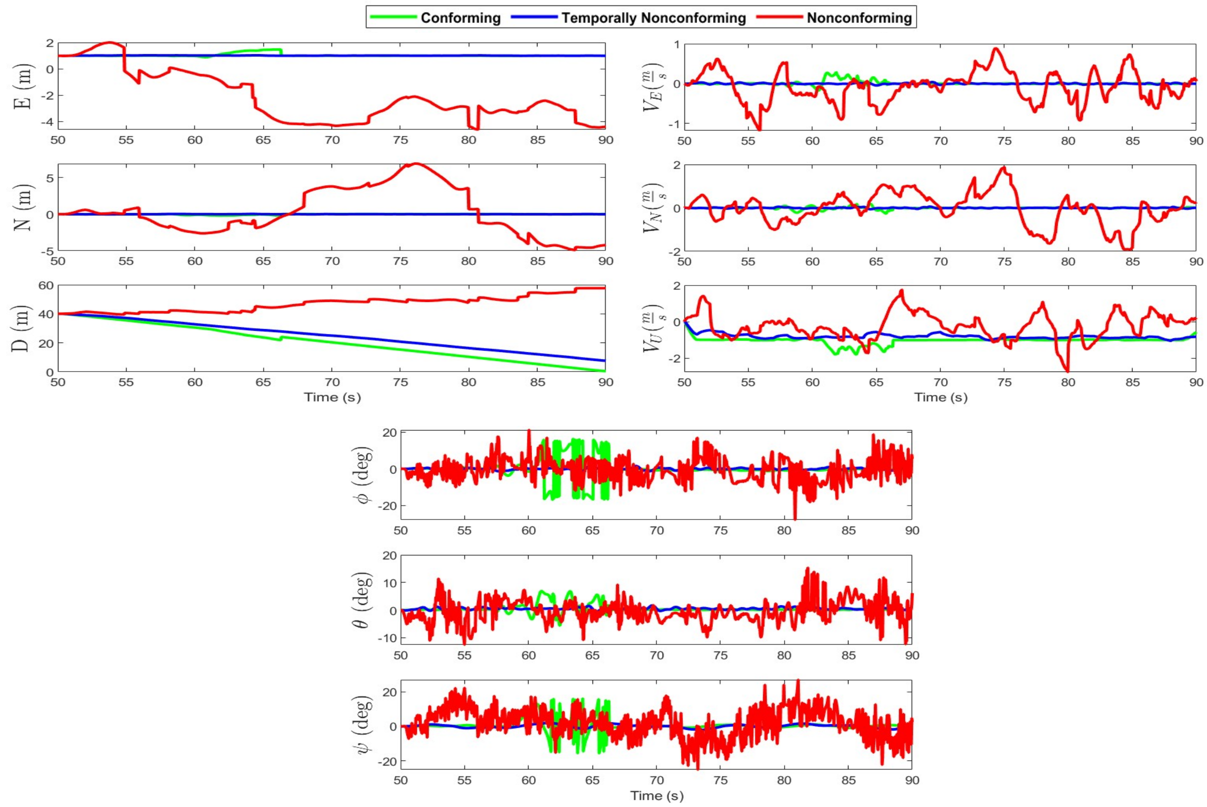

Figure 6. Time series plots of mean aircraft position, velocity, and attitude of conforming, temporally non-conforming, and non-conforming cases.

grees. Whilst for the critical LOC instances, it can be noticed that the wind flows from the directions between 300 and 60 degrees with wind speed ranging from 5 to 20 m/s. This signifies severe headwind oriented towards the negative Y-axis of the simulation domain, contributing to the controller saturation observed in these cases.

Given that LOC cases represent full control saturation with unrecoverable states, it was deemed unnecessary to assess trajectory deviations for these instances. Consequently, the analysis of trajectory deviations was focused on the remaining flight scenarios–conforming, temporally non-conforming, and non-conforming cases. These scenarios were clustered accordingly, and the mean time series of position, velocity, and attitude data was computed for each group to offer insights into the representative dynamic behavior of the aircraft across the 3 trajectory classes (see Figure 6).

As expected, the non-conforming cases exhibit the most significant deviations in position compared to the conforming and temporally non-conforming instances. Notably, the aircraft in non-conforming scenarios tend to drift predominantly towards the West (negative x-axis), where the building is assumed to be present. Concurrently, a lateral shift towards the north (positive y-axis) is also observed. These spatial deviations align with prior findings, which identified the incident wind direction for non-conforming cases to be between 90 and 270 degrees – i.e., tail or crosswind. The vertical position of the aircraft remains consistently above 40 meters. This suggests that the aircraft may either be hovering as the controller attempts to compensate for wind-induced disturbances for some iterations, or experiencing upward displacement due to strong updrafts. Furthermore, it is important to emphasize that some instances within the non-conforming group showed substantial variability in displacement with max displacement exceeding 50 m (see the non-conforming plot in Figure 4).

For both the conforming and temporally non-conforming cases, the horizontal and lateral velocities remain close to zero throughout the majority of the descent, with only minor deviations occurring after the initial 20 seconds of flight. These disturbances are likely due to sudden gusts of wind and the corresponding transient response from the controller. Nevertheless, these deviations are minimal and do not significantly impact the overall trajectory. Similarly, the mean descent velocity in the conforming cases is maintained at 1.2 m/s, whereas temporally non-conforming cases show a lower mean descent velocity of approximately 0.8 m/s. This reduced descent rate explains why the vertical position of the aircraft in this class remains at altitudes greater than 1 meter by the end of the designated 90 s total flight time (see position plot in Figure 6). In contrast, the non-conforming cases display substantial fluctuations in velocity across all three axes, indicating instability in the descent profile and insufficient control authority against the inflow wind.

A trend similar to that of the aircraft position and velocity is also evident in the attitude behavior across the 3 trajec-

Table 1. Mean attitude statistics for the conforming, temporally non-conforming, and non-conforming trajectory classes.

	Roll, ϕ (deg)	**Pitch,** θ (deg)	**Yaw,** ψ (deg)
Conforming			
Mean[a]	2.9	0.9	1.1
Std dev.(±)[b]	8.8	2.4	7
Maximum[c]	7.8	7.7	11.9
Temporally non-conforming			
Mean	2.5	1.1	0.3
Std dev.(±)	1.7	0.9	3.1
Maximum	4.8	2.5	0.6
Non-conforming			
Mean	10.5	2.4	9.4
Std dev.(±)	30.8	19	39.9
Maximum	26.6	11.2	86.8

[a]Mean values across all trajectories in each class. [b]Standard deviation values across all trajectories in each class. [c]Maximum values observed across all trajectories in each class.

tory classes. Specifically, both the conforming and temporally non-conforming cases exhibit relatively small variations in roll, pitch, and yaw, whereas the non-conforming cases demonstrate significantly larger deviations across all 3 axes. This observation is further substantiated by the statistical data presented in Table 1, which reveals noticeably higher variability in roll and yaw compared to pitch. Such discrepancy implies that the controller is less effective in mitigating the wind disturbances along the roll and yaw axes, suggesting that the lateral control must be tuned to better counter the lateral-directional coupling effects.

A contrasting observation to the overall pattern of the 3 classes observed in Table 1 is that the conforming cases exhibit slightly higher standard deviations in attitude than the temporally non-conforming cases. This difference could be attributed to transient fluctuations occurring shortly after the initial 20 seconds of descent–a pattern that is also visualized in the position and velocity plots. These brief disturbances may have skewed the statistical measures for the conforming cases, resulting in a higher overall standard deviation despite the controller maintaining a stable attitude throughout the remainder of the descent.

Overall, the trajectory analysis shows that conforming cases typically occur under milder incidence wind conditions, while non-conforming trajectories are associated with stronger crosswinds or headwinds and adverse outcomes such as instability, delayed descent, and increased variability in position, velocity, and attitude. These results are consistent with theoretical expectations, reinforcing that microscale wind-induced disturbances significantly challenge controller performance during vertical descent. Additionally, this analysis also highlights limitations in the ability of the controller to mitigate such disturbances.

Determination of wind disturbance levels

While the trajectory analysis offered useful insights into the dynamic behavior of the aircraft across different conformance classes, it did not fully quantify the wind disturbance levels responsible for the observed conformance non-compliance. Thus, to characterize these disturbances, this section explores the probability distributions of inflow wind speed, direction, and the aircraft deviations relative to the identified inflow conditions, employing Kernel Density Estimation (KDE) and Cumulative Distribution Functions (CDFs) (Refs. 21, 22).

Figure 7 presents the distribution of mean inflow wind velocity magnitude and direction (measured at aircraft CG) for each conformance class. For the conforming case, wind speeds are predominantly between 0 and 1 m/s, with directions ranging from 60 to 120 degrees, indicating a high likelihood of mild crosswind conditions centered around 0.6 m/s across all iterations. In contrast, the temporally non-conforming cases exhibit slightly higher wind velocities, ranging from 1 to 2 m/s, with wind directions predominantly between 90 and 150 degrees. This suggests a consistent exposure to a modest crosswind combined with a tailwind component, with wind speeds clustering around 1.5 m/s. The non-conforming cases, however, show a much flatter and broader wind velocity distribution, spanning from 2 m/s to 6 m/s. This indicates that the aircraft in this class encounters a wider range of rapidly varying wind conditions. These findings align with the increased fluctuations in the mean position, velocity, and attitude observed in the trajectory analysis for non-conforming cases. Wind direction in this group ranges from 40 to 120 degrees, implying the presence of either pure crosswind or a combination of headwind and crosswind components. Furthermore, the mean turbulence intensity for the conforming, temporally non-conforming, and non-conforming classes was found to be approximately 14%, 16%, and 65%, respectively. The significantly higher turbulence intensity in the non-conforming cases could be owed to the increased wind velocity and variability.

The cumulative probability of mean lateral and vertical deviation plots (see Figure 8) suggests that for both the conforming and temporally non-conforming cases, the probability of the aircraft experiencing minor lateral deviations is remarkably high. In the lateral deviation plot, both lines rise steeply around zero, indicating that for these scenarios, deviations are predominantly in the decimal range, with nearly 100% of deviations being less than 0.5 m. A similar trend is also visible in the vertical deviation plot for these two cases, where deviations are tightly clustered around zero. Specifically, for the conforming case, it can be inferred that there will be less than 0.5-1.0 m vertical deviation for 99% of the time. For the temporally non-conforming case, there is a slight shift towards the right when compared to the conforming case. This implies that the aircraft will experience about 4.5 m of vertical deviation for 50% of the time, and less than 10 m of deviation for 99% of the time. On the whole, this suggests that for the conforming and temporally non-conforming flights, the lateral and vertical deviations are minimal, indicating a well-

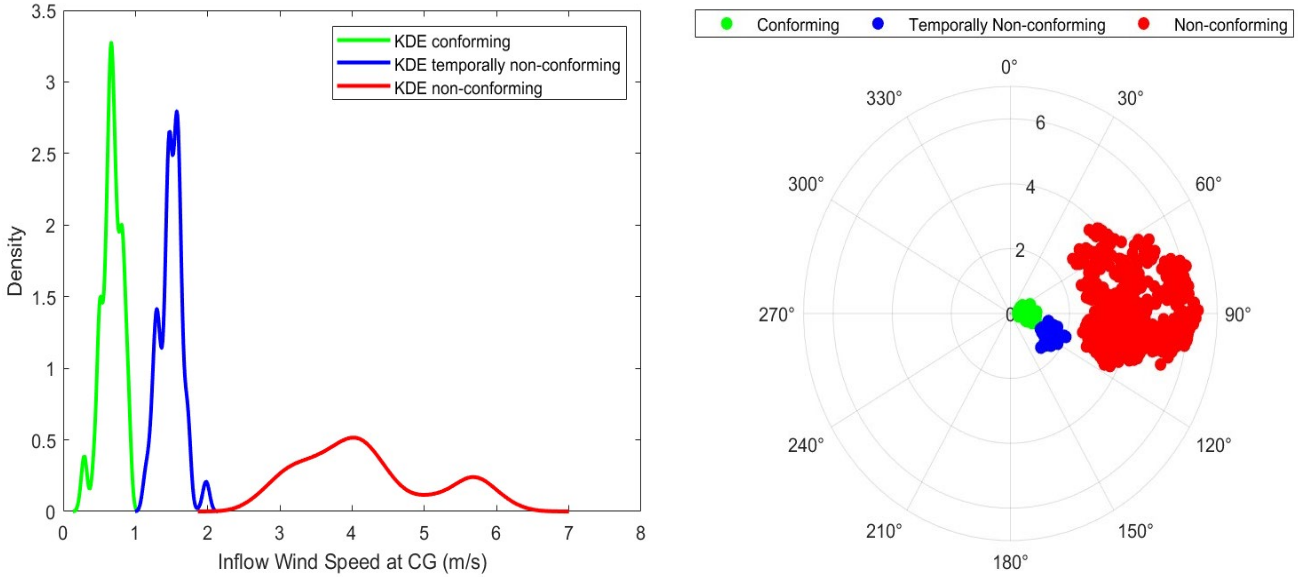

Figure 7. (Left) Wind speed distributions at CG for the 3 trajectory categories, estimated via KDE; (Right) Inflow wind speed and direction at CG classified under the conformance classes.

established control authority.

On the other hand, the non-conforming class displays a considerably higher likelihood and widespread intensity of both lateral and vertical deviations. In the lateral deviation plot, the deviation extends up to 20 meters for the 90th percentile and around 29-42 meters for the 99th percentile. Similarly, in the vertical deviation plot for the non-conforming case, the 90th percentile deviation is about 36 meters. Additionally, both the lateral and vertical distribution plots exhibit a pronounced positive skew, indicating a higher tendency for the aircraft to deviate in the positive direction–laterally to the right and vertically upward.

Furthermore, the mean lateral deviation values corresponding to the 3 trajectory classes are filtered based on their associated mean inflow wind speed intervals (minimum to maximum values within each class) and used to construct Empirical Cumulative Distribution Functions (ECDFs) (Ref. 23). This is done primarily to quantify wind disturbance levels for the UAM aircraft under consideration. Figure 9 indicates that for wind speeds between 0.24 m/s and 2.01 m/s, lateral deviation remains below 1.5 m for 99% of the observations. Whereas for wind speeds exceeding 2.5 m/s, the likelihood of larger deviations increases significantly, with values reaching up to 8 m for 50% of cases and approaching around 14 meters for 99%. Altogether, these results demonstrate a distinct wind speed threshold beyond which lateral instability becomes highly probable.

Based on the statistics from this analysis, a wind disturbance classification table and a Minimum Acceptable Handling Qualities [2] Rating (MHQR) table for the eVTOL drone and flight phase under study–with coherent definitions for each wind disturbance level–can be constructed (see EASA's Means of Compliance with SC-VTOL, Table 2: Minimum Acceptable Handling Qualities Rating and Table 4: Probability of Occurrence Guidelines for Atmospheric Disturbance Level (AD) (Ref. 24)). However, it is important to note that the figures presented in this analysis reflect only the flight simulator performance, not that of the actual aircraft. That is, the outcomes are dependent on the fidelity of the flight simulator, including the controller and dynamics model implemented, as well as the reliability of the SWM-derived microscale wind conditions. Therefore, a validation study using experimental data and uncertainty analysis is essential to accurately establish the critical values and ensure their applicability in real-world scenarios.

CONCLUSIONS

This paper presents an efficient simulation-based methodology that integrates a UAM aircraft flight simulator and a custom microscale wind model within a Monte Carlo framework to quantify wind disturbance levels and assess the degradation of handling qualities (HQ). The methodology is demonstrated through a case study involving the vertical landing of an eVTOL behind an isolated building, with 100 Monte Carlo simulations conducted by varying the incident wind speed and direction within the simulation domain. The resulting trajectory data from all iterations are aggregated and categorized into 4 conformance classes: Conforming, Temporally Non-Conforming, Non-Conforming, and Loss of Control (LOC).

[2]In this paper, “Handling Qualities” refers to how well the drone responds to control inputs or automated commands, and how effectively it maintains stable and desired behavior in various flight conditions.

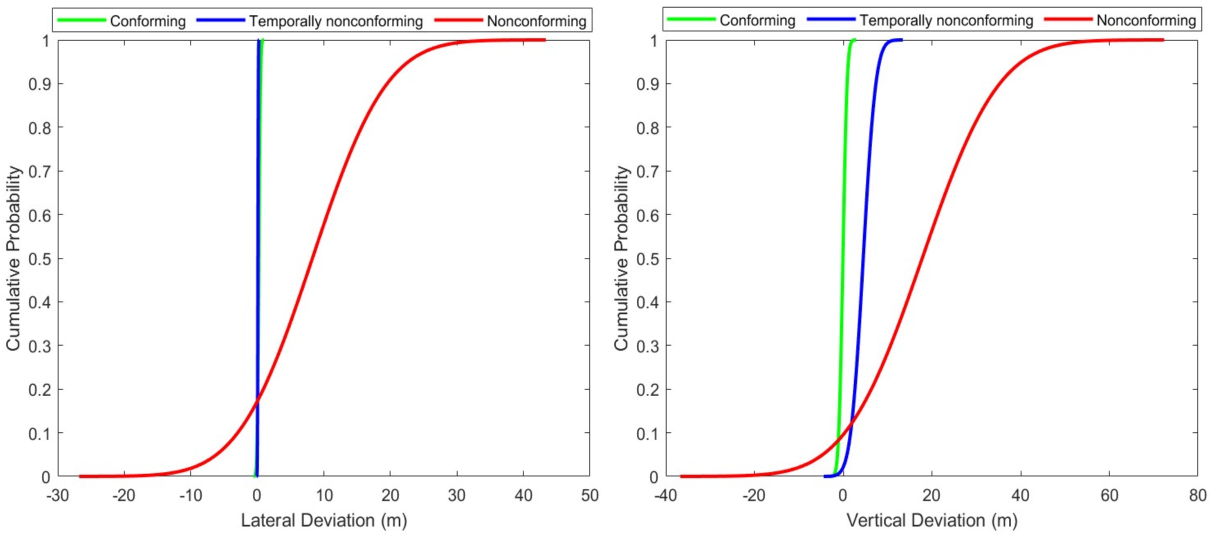

Figure 8. Cumulative distribution of lateral and vertical deviations during descent for the 3 classified conformance categories.

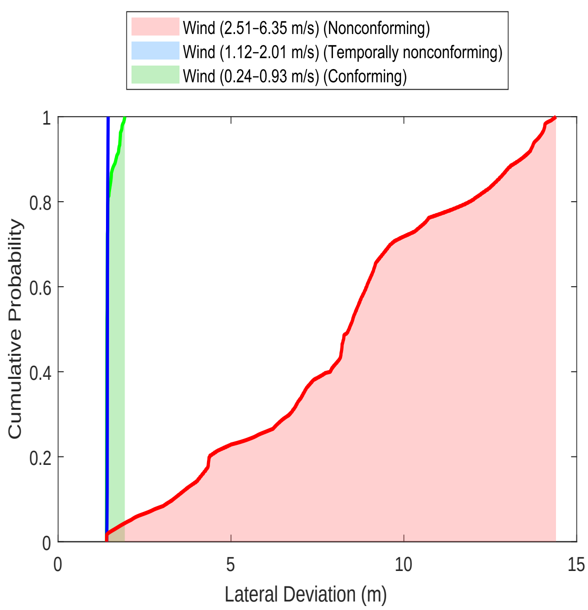

Figure 9. Empirical cumulative distribution of lateral deviation relative to inflow wind speed for the conforming, temporally non-conforming, and non-conforming classes.

Of the 100 simulated flights, 41 were classified as LOC, reducing the number of cases analyzed for trajectory deviation to 59. The mean position, velocity, and attitude data–of those iterations falling under the conforming, temporally non-conforming, and non-conforming categories–were analyzed to characterize the inflow wind conditions and associated flight dynamics. This analysis reveals that non-conforming trajectories exhibit degraded controller performance, marked by significant roll-yaw coupling, large lateral and vertical deviations, and rapid velocity fluctuations–indicative of trajectory instability during descent. Furthermore, the positional deviations were correlated with inflow wind speed and direction, allowing the identification of 3 distinct wind velocity and direction ranges associated with each trajectory class. The probability and magnitude of these deviations were quantified as functions of inflow wind conditions, enabling the linkage of wind disturbance levels to trajectory deviation risk. However, a limitation of the methodology lies in its reliance on the fidelity of the flight simulator—including the controller and dynamics model—and the accuracy of the SWM in reproducing realistic microscale wind conditions.

Future work should aim to enhance the fidelity of the simulation framework, quantify uncertainties and perform validation using experimental data. Additionally, explicit assessments of controller response range should be incorporated to directly link wind disturbances to HQ degradation beyond trajectory deviations. The methodology should also be extended to a wider range of UAM aircraft configurations and urban operational scenarios to provide a more comprehensive understanding of aircraft performance risks within the urban low-altitude atmosphere.

To conclude, the methodology proposed in this paper provides an initial understanding of the landing trajectory deviation risks that UAM aircraft may experience due to microscale wind disturbances in the vicinity of a building. Ultimately, this approach can be leveraged to quantify wind disturbance levels in support of UAM aircraft certification efforts, assist in the design of robust aircraft, controllers, and flight simulators, and define the operational safety-critical limits of the aircraft in a more cost-effective and time-efficient way than traditional flight test campaigns.

Authors' contact:
Nithya D S nithya.dhamodharasamy@polimi.it
Agata Rylko agata.rylko@polimi.it
Vincenzo Muscarello vincenzo.muscarello@rmit.edu.au
Man Liang man.liang@rmit.edu.au
Giuseppe Quaranta giuseppe.quaranta@polimi.it

ACKNOWLEDGMENTS

This research is conducted under the REDI (RMIT European Doctoral Innovators) Program. This project has received funding from the European Union's Horizon 2020 research and innovation programme under the Marie Skłodowska-Curie grant agreement no. 101034328.

REFERENCES

1. Mohamed, A., Marino, M., Watkins, S., Jaworski, J., and Jones, A., "Gusts Encountered by Flying Vehicles in Proximity to Buildings," *Drones*, Vol. 7, 22, 2023.

2. Nithya, D. S., Quaranta, G., Muscarello, V., and Liang, M., "Assessment of a highly parameterized steady-state microscale wind simulator for urban air mobility applications," 31st Congress of the International Council of Aeronautical Sciences, 2024.

3. EASA, *Third Publication of Means of Compliance with the Special Condition VTOL (MOC-3 SC-VTOL), Issue 2*, European Union Aviation Safety Agency (EASA), 21 June 2023.

4. Nithya, D. S., Quaranta, G., Muscarello, V., and Liang, M., "Review of Wind Flow Modelling in Urban Environments to Support the Development of Urban Air Mobility," *Drones*, Vol. 8(4), 147, 2024.

5. Banerjee, P., Corbetta, M., Jarvis, K., Smalling, K., and Turner, A., "Probability of Trajectory Deviation of Unmanned Aerial Vehicle in Presence of Wind," *Journal of Air Transportation*, Vol. 31, 3, 2023.

6. Krammer, C., and Holzapfel, F., "Estimation of Probability of Exceeding SC-VTOL Performance Requirements During Automatic Landing Using Subset Simulation," 79th Vertical Flight Society Annual Forum & Technology Display, 2023.

7. Vuppala, R. K. S. S., Krawczyk, Z., Paul, R., and Kara, K., "Modeling advanced air mobility aircraft in data-driven reduced order realistic urban winds," *Sci Rep*, Vol. 14, 383, 2024.

8. Brown, M. J., Williams, M. D., Nelson, M. A., and Werley, K. A., "QUIC transport and dispersion modeling of vehicle emissions in cities for better public health assessments," *Environmental Health Insights*, 2015.

9. Bozorgmehr, B., Patterson, Z., Willemsen, P., Margairaz, F., Gibbs, J., Stoll, R., and Pardyjak, E. R., "UtahEFD/QES-Public [Computer Software]," , June 2024.

10. Kelley, N., and Jonkman, B., "Overview of the TurbSim stochastic inflow turbulence simulator," Technical Report Version 1.21, National Renewable Energy Laboratory (NREL), Golden, CO, United States, 2007.

11. Nithya, D. S., Rylko, A., Muscarello, V., Liang, M., and Quaranta, G., "Effects of Microscale Wind Disturbance on eVTOL Aircraft Performance During Landing," 50th European Rotorcraft Forum (ERF), 2024.

12. Nithya, D. S., Muscarello, V., Liang, M., and Quaranta, G., "Sensitivity Analysis of Urban Air Mobility Aircraft Landing Trajectory Deviation to Microscale Wind Disturbances," 81st International Annual Forum Vertical FLight Society (VFS), 2025.

13. European Union Aviation Safety Agency, "Prototype Technical Specifications for the Design of VFR Vertiports for Operation with Manned VTOL-Capable Aircraft Certified in the Enhanced Category (PTS-VPT-DSN)," Technical report, EASA, March 2022.

14. Martello, N. C., *Modelling and integration of an eVTOL UAV*, Master's thesis, Politecnico di Milano, Italy, 2021.

15. Battaini, N., *Design and dynamic modeling of a VTOL UAV*, Master's thesis, Politecnico di Milano, Italy, 2019.

16. Martinelli, E., *Modelling, control, integration and testing of an eVTOL drone*, Master's thesis, Politecnico di Milano, Italy, 2022.

17. Bara, K., *Aerodynamics, propulsion and testing of an eVTOL drone*, Master's thesis, Politecnico di Milano, Italy, 2023.

18. Abbate, S., *Trajectory tracking control design for eVTOL UAVs with input redundancy optimization*, Master's thesis, Politecnico di Milano, Italy, 2023.

19. Marchesi, M., *Structural redesign, simulation, control, and state estimation of an eVTOL UAV*, Master's thesis, Politecnico di Milano, Italy, 2024.

20. Willis, J. B., *Trajectory generation and tracking control for winged electric vertical takeoff and landing aircraft*, Master's thesis, Brigham Young University, 2021.

21. Silverman, B. W., *Density Estimation for Statistics and Data Analysis*, Chapman and Hall, 1986.

22. Casella, G., and Berger, R. L., *Statistical Inference*, Duxbury Press, second edition, 2002.

23. MATLAB, *ecdf - Empirical cumulative distribution function*, The MathWorks, Inc., 2024.

24. EASA, *Means of Compliance with the Special Condition VTOL (MOC SC-VTOL), Issue 2*, European Union Aviation Safety Agency (EASA), 12 May 2021.